Shipman et al. A protective Langerhans cell-keratinocyte axis that is dysfunctional in photosensitivity

SUPPLEMENTARY MATERIALS AND METHODS

Mice

Mice from 6-12 weeks old were used unless otherwise stated and were sex and aged-matched. Both male and female mice were used for experiments, except for B6.Sle1yaa mice, in which only males were used because the model is dependent in part on the autoimmune accelerator locus on the Y chromosome (*40*). C57BL/6J, Langerin-DTA, $Rag1^{-/-}$, Balb/c, MRL-MpJ, MRL-*Fas*^{lpr}, and B6.Sle1yaa mice were originally from Jackson Laboratory (JAX) and bred at our facility. CCR2-GFP and CCR2-DTR mice (*25*) were bred at our facility. $Rag1^{-/-}$ mice were intercrossed with Langerin-DTA mice to generate $Rag1^{-/-}$ Langerin-DTA mice. $ADAM17^{flox/flox}$ mice (*32*) were intercrossed with Langerin-$Cre^{+/-}$ mice (*33, 34*) (National Cancer Institute (NCI)), and Langerin-$Cre^{ER+/-}$YFP mice (*34*) to generate LC-Ad17 and Langerin-$Cre^{ER+/-}ADAM17^{flox/flox}$ mice, respectively. The WT mice used in experiments involving LC-Ad17 mice were Langerin-$Cre^{-/-}$ $ADAM17^{flox/flox}$ littermate controls. All animal procedures were performed in accordance with the regulations of the Institutional Animal Use and Care Committee at the Hospital for Special Surgery and Weill Cornell Medicine.

Human research participants

For immunofluorescence analysis, non-sun-exposed nonlesional skin from the buttocks of healthy controls and SLE patients was used. With the exception of one healthy control, all skin samples were from samples examined in (*53*). Controls were between the ages of 28-65 and 67% were female. The SLE patients met American College of Rheumatology criteria for SLE, were between the ages of 19-62 years old, and 79% were female. All SLE patients were

currently receiving treatment at the time of the biopsy (*53*). These samples were collected and used in accordance with the Institutional Review Board at the NYU School of Medicine (IRB# S14-00487).

For human LC and epidermal CD45+ non-LC cell isolation, human skin samples were collected from eleven human patients undergoing elective reconstructive surgery at the Division of Plastic and Reconstructive Surgery at the Memorial Sloan Kettering Cancer Center (MSKCC). Ten of the eleven patients were female and the patients were between the ages of 41-69 at the time of surgery. All tissue collection and research use adhered to protocols approved by the Institutional Review and Privacy Board at the Memorial Sloan Kettering Cancer Center, and all participants signed written informed consents (IRB# 06-107).

Mouse treatments

For indicated 24 hour experiments, HB-EGF (2ug; R&D Systems) dissolved in dimethyl sulfoxide (DMSO) was applied to each ear 15 minutes prior to UVR exposure. For long-term lesion development experiments, mice were shaved in a small area on the lower back. At 24 hours, HB-EGF was applied on the ears as above and on the shaved back area (8ug) for three consecutive days. Mice received their first dose of UVR on the last day of HB-EGF treatment.

Flow cytometry, cell sorting, and quantification

For staining of murine whole skin, single cell suspensions of skin were generated as previously described (*14*). Briefly, ear skin was excised, finely minced, digested in collagenase type II (616 U/mL; Worthington Biochemical Corporation), dispase (2.42 U/mL; Life Technologies),

and DNAse1 (80 μg/mL; Sigma-Aldrich), incubated at 37°C while shaking at 100 rpm, triturated with glass pipettes, and filtered. For murine epidermal cell staining or sorting, ear and trunk skin was incubated in dispase at 37°C for 45 minutes. The epidermis was then scraped off and finely minced before digestion in collagenase type II.

For flow cytometry analysis, the following gating strategies were used after excluding debris and non-single cells: *LCs:* Lineage(CD3, B220, NK, Ly6G)-, CD45+ CD11b+ CD24+, CD11c+, MHCII+; *monocytes*: Lineage-, CD45+, CD11b+, CD24-, Ly6C+, MHCII-; *monocyte-derived DCs*: Lineage- CD45+ CD11b+ CD24- $Ly6C^{hi-lo}$, MHCII+; *CD11b+ DCs*: Lineage- CD45+ CD24- CD11b+ Ly6C- CD64- CD11c+ MHCII+; *CD11b- DCs*: Lineage- CD45+ CD11b- CD24+ CD11c+ MHCII+; *macrophages:* Lineage- CD45+ CD11b+ CD24- CD64+; *neutrophils:* Lineage+ CD11b+ $Ly6C^{med}$, side scatter $(SSC)^{hi}$; *T cells*: epidermal CD45+, CD11b-, CD3+; *keratinocytes*: epidermal CD45-, CD31-, EpCAM+ or total skin CD45-, CD31-, CD49f+, Sca1+, EpCAM+; *skin plasma cells*: CD45+, $B220^{lo}$, CD3-, intracellular IgG^{hi}; *lymph node germinal center B cells*: CD3-, B220+, PNA+; *lymph node plasma cells:* CD3-, $B220^{lo}$, CD138+. LCs, monocytes, monocyte-derived DCs, CD11b+ DCs, CD11b- DCs, and macrophages were gated according to Tamoutounour et al. (*24*). Primary and secondary antibodies are described in Table S1 and Table S2.

For flow cytometry analysis, cells were analyzed using a FACSCanto (BD Biosciences) and FlowJo Software (Tree Star). Cells were sorted using a BD Influx.

To measure phosphoEGFR by flow cytometry, cells were serum- or EGF-starved, pretreated with 2 mM $NaVO_3$ for 15 minutes, fixed with 4% paraformaldehyde for 15 minutes at room temperature, and then permeabilized with ice-cold methanol (90%) for 30 minutes on ice. The cells were then stained with anti-phosphoEGFR Tyr1068 (Cell Signaling) followed by anti-rabbit Alexa647 (Jackson Immunoresearch).

For isolation of murine epidermal cells for cultures and qPCR, epidermal single cell suspensions from ear and back skin were flow sorted for CD45+CD11b+ EpCAM+ CD3- LCs, CD45+CD3+CD11b- T cells, and CD45-, CD31-, EpCAM+ keratinocytes. Purity of sorted cells was >95%.

For human LC and CD45+ non-LC isolations, fresh skin samples were obtained from patients undergoing elective reconstructive surgery as described above. Skin samples were cut into small pieces and incubated for 30 min at 37°C and 5% CO_2 in prewarmed DMEM/F-12 (Stem Cell Technologies) with dispase II (1 IU/ml; Roche Diagnostics) to facilitate separation of the epidermis from the dermis. The epidermis was gently peeled away from the dermis and placed in RPMI 1640 supplemented with 10 mM HEPES, 1% penicillin/streptomycin (Media Lab, MSKCC), 50 mM L-glutamine (Cellgro), 50 μM β-mercaptoethanol (Gibco, Life Technologies), and 10% heat-inactivated pooled healthy human serum (Atlanta Biologicals). The epidermal sheets were then finely minced and digested with collagenase as described for mouse epidermis. LCs (CD45+ CD1a+ HLADR+), non-LC CD45+ cells (CD45+ CD1a- HLADR-), T cells (CD45+ CD1a- HLADR- CD3+), and keratinocytes (CD45- CD1a- CD3- EpCAM+) were sorted and sorted cells had a purity ≥ 95%.

Human epidermal cells used for flow cytometric analysis of ADAM17 were incubated with human TruStain FcX Fc receptor blocking solution (BioLegend), the cells were then stained with anti-human ADAM17 (Abcam) or human IgG1 isotype control (Adipogen), followed by anti-human IgG biotin (Jackson Immunoresearch) and streptavidin Alexa 488 (Thermo Fisher Scientific- Invitrogen). After excluding debris, dead cells, and non-single cells the following gating strategies were used to examine ADAM17 expression: LCs: CD45+ CD1a+ HLADR+ CD3-, T cells: CD45+ CD3+ CD1a- HLADR- and keratinocytes: CD45- CD1a- HLADR- EpCAM+.

Cells were counted using a Z1 Coulter Counter (Beckman Coulter). To calculate absolute cell numbers, the percentage of the total of a particular population was multiplied by the total cell count from the Coulter Counter. For figures showing normalized values, the control sample was set to 1, and the experimental samples were normalized relative to the control for that experiment. For experiments that contained more than one control sample, the mean was obtained for the control samples, and the individual control and experimental samples were calculated relative to this mean.

Histology, immunofluorescence staining, and quantifications

For immunofluorescence staining of murine skin, frozen unfixed mouse skin was sectioned, fixed with cold acetone for 10 minutes, and stained as indicated (*15*). Epidermal activated caspase-3+ cells per high powered field (40x magnification) were quantified by a blinded observer using ImageJ software (NIH) and classified as activated caspase-3+ keratinocytes (Langerin- and CD3-), LCs (Langerin+), or T cells (CD3+).

Formalin-fixed paraffin embedded murine skin was stained with hematoxylin and eosin, and epidermal thickness was measured by a blinded observer using ImageJ software.

For immunofluorescence staining of cell culture experiments, polystyrene chamberslides (Lab-Tek) with cultured keratinocytes were washed with PBS, fixed with 4% paraformaldehyde for 20 minutes, permeabilized and blocked with Triton-X (0.2%) and BSA (1%), and stained as indicated. Activated caspase-3+ and total DAPI+ cells were quantified with ImageJ software by a blinded observer and the percent of activated caspase-3+ Langerin- cells (keratinocytes) and activated caspase-3+ Langerin+ cells (LCs) was calculated.

For immunofluorescence staining of human skin, formalin-fixed paraffin-embedded tissue sections were rehydrated and underwent antigen retrieval at 60°C in 10 mM citrate buffer, pH

6.0 for 20 hours followed by enzymatic retrieval with Carezyme III: Pronase Kit (Biocare Medical) for 15 minutes. Sections were then stained as indicated. The fluorescence intensity of phosphoEGFR and total EGFR was measured using ImageJ software and the fluorescence intensity of the isotype control was subtracted. The ratio of phosphoEGFR:total EGFR was then calculated and normalized to the ratio for the healthy control samples that were stained at the same time as the SLE samples. Langerin+ cells in the epidermis were counted by a blinded observer using ImageJ software and normalized to the length of the tissue.

All antibodies and staining reagents are described in Table S1 and Table S2. Histology was imaged using either a Nikon Eclipse E600 with a Q-Imaging Retiga Exi camera or a Nikon Eclipse NI-E Fluorescence Upright microscope coupled to a Zyla sCMOS camera (Andor Technology).

Western blots

Western blots were performed essentially as described (*23*). Ears were harvested and the epidermis was isolated by incubating skin in distilled water at 60 °C for 20 seconds and then in ice cold PBS for 20 seconds before the epidermis was gently scraped off. Epidermal sheets were then lysed on ice with a Polytron PT 10-35 tissue homogenizer in lysis buffer (50 mM Tris-HCl pH 7.7, 1% Triton-X, 150 mM NaCl, 1 mM EDTA, 10 mM NaF, 5 mM β-glycerophosphate, 2 mM $NaVO_3$, 1 mM 1,10-ortho-phenanthroline (Sigma-Aldrich), and protease inhibitor cocktail set III (EMD Millipore)). Samples (10-15 µg protein) were separated on a 10% SDS-polyacrylamide gel, transferred to nitrocellulose paper, and Western blots were then stained as indicated. Antibody staining was detected using ECL Plus Western blotting substrate (Thermo Fisher Scientific). Blots were first stained for phosphoEGFR, stripped with 1 M Tris pH 6.75, β-mercaptoethanol, and SDS at room temperature followed by incubation at 60

°C, and then reprobed for total EGFR. All antibodies used for Western blots are described in Table S1 and Table S2. Western blots were quantified with ImageJ software and the ratio of phosphoEGFR: total EGFR was determined and normalized to the ratio of the control samples.

Epidermal permeability measurement

Toluidine blue dye penetrance was measured essentially as described (*23*). Dehydrated and rehydrated ear skin was incubated for 2 min in 0.1% toluidine blue dye (Sigma-Aldrich) before destaining and toluidine blue dye extraction with a solution of 2.5% H_2SO_4, 2.5% H_2O, and 95% methanol. Colorimetric values were measured at 620 nm and the total amount of toluidine blue dye was calculated using the volume of extraction solution, which was constant among the conditions.

In vitro experiments

Mouse keratinocyte-LC co-cultures:

Primary mouse keratinocyte cultures were prepared from mouse tail skin as described (*23*). The isolated epidermal cells were plated in 8-well chamberslides (Lab-Tek) coated with 7 ng/μL collagen I (BD Biosciences) at 2-4 x 10^5 cells per well in serum-free keratinocyte growth media 2 (KGM2) (PromoCell). 3-4 days later, keratinocytes were at 90% confluency and sorted LCs were added at a density of 20,000-25,000 LCs per well. The co-cultures rested overnight and were then exposed to UVR and analyzed 24 hours later. Unless indicated, co-cultures were exposed to UVR in approximately 200 μL of minimally colored culture media containing 3.3 mM phenol red and without a plastic covering.

Keratinocyte EGFR knockdown co-cultures:

Primary mouse keratinocytes were cultured as described above and, at 40-50% confluency, were treated with control siRNA or two different EGFR siRNAs (siRNA #1 or #2) (Accell siRNA from Dharmacon, GE Lifesciences) according to the manufacturer's protocol. Target sequences of the siRNAs were: siRNA #1- 5'-GAUUGGUGCUGUGCGAUUC-3' and siRNA #2- 5'-GCAUAGGCAUUGGUGAAUU-3'. The media was changed to normal keratinocyte growth media on day 4, and the co-culture experiments were subsequently conducted as described in Materials and Methods in the main text. Separate wells on the same chamberslides were collected on day 5 (the day of UVR exposure) to check efficiency of EGFR knockdown by flow cytometry.

Keratinocyte PD168393 treatment co-cultures:

Primary mouse keratinocytes were treated with 2 μM PD168393 (Cayman Chemicals), an irreversible EGFR inhibitor, for 30 minutes. The PD168393 was washed off with PBS and fresh keratinocyte growth media was supplied with or without LCs and the co-culture experiments were subsequently conducted. Keratinocytes from separate wells were collected at the time of co-culture and treated with EGF (200 ng/mL) to validate the efficiency of EGFR inhibition by measuring phosphoEGFR by flow cytometry.

Human keratinocyte-LC co-cultures:

Primary human keratinocytes (Lonza) were prepared according to the manufacturer's protocol and plated on collagen-coated chamberslides at 1-2 days before use. Human LCs and non-LC CD45+ cells were sorted from epidermis and added to 50-90% confluent keratinocyte cultures at 16,000-20,000 cells per chamberslide well. The co-cultures were rested overnight, exposed

to UVR, and examined 24 hours after UVR. Some wells of keratinocytes were treated with recombinant human HB-EGF (R&D Systems) at indicated concentrations, rested overnight, and then exposed to UVR. For anti-ADAM17 blocking experiments, LCs were pretreated with 200 nM of anti-human ADAM17 blocking antibody (Abcam) or human IgG1 isotype control antibody (Adipogen) for 30 minutes before they were added with the antibodies to the keratinocytes. Anti-ADAM17 blocking antibody and IgG1 isotype control antibody was also included in keratinocyte cultures without LCs as additional controls.

Ex vivo ADAM17 activity assay by TNFR1 cleavage

Sorted mouse LCs were plated in a 96-well plate at 20,000-25,000 cells/well in RPMI 1640 supplemented with L-glutamine, penicillin/streptomycin, and HEPES buffer. The cells were treated with phorbol 12-myristate 13-acetate (PMA) (Sigma-Aldrich) at 25 ng/mL or UVR (500 J/m^2) and analyzed 45 minutes later. The cells were then stained with DAPI to exclude dead cells and for cell-surface TNFR1 (BioLegend). ADAM17 activity is expressed as the percent change in TNFR1 mean fluorescence intensity (MFI) relative to that of untreated LCs. Sorted human LCs (3,000-5,000 cells/well) were plated and treated with anti-ADAM17 blocking antibody or human IgG1 isotype control antibody for 30 minutes prior to UVR exposure and analysis of TNFR1 MFI. For collection of conditioned supernatant from sorted human LCs to add to A431 cells, 1,500 LCs were treated with IgG control or anti-ADAM17 blocking antibody for 30 minutes, washed, and then transferred into new media prior to UVR treatment to prevent carryover of blocking antibodies into the conditioned supernatant.

EGFR ligand release assay with A431 indicator cells

A431 human squamous carcinoma cells (ATCC) were cultured according to the manufacturer's protocol in 96 well plates. At about 80% confluency, the A431 cells were serum-starved overnight then pretreated with 2 mM $NaVO_3$ for 15 minutes at 37° C, and were then treated with conditioned supernatants from various cells for 10 minutes. The A431 cells were then collected and phosphoEGFR expression was measured by flow cytometry. All experiments were conducted with A431 cells in passage 2.

Lesion quantification

The remaining hair on the back skin of the mice was removed using Nair and photographs were taken. The total back area and lesional area (skin affected by erythema, scaliness, crustiness, or epidermal erosion) was measured by a blinded observer using ImageJ software and skin lesions were quantified as percent of back area.

mRNA quantification

Cells were sorted directly into RLT lysis buffer (Qiagen) with β-mercaptoethanol (Bio-Rad) and stored at -80°C until RNA extraction with Qiagen RNeasy Mini Kit. cDNA was generated using iScript cDNA synthesis kit (Bio-Rad) and real-time PCR was performed using iQ SYBR Green Supermix kit (Bio-Rad) on a Bio-Rad MyiQ thermal cycler or Maxima SYBR Green/ROX qPCR Master Mix (Thermo Fisher Scientific) on a StepOne Plus Real-Time PCR system (Applied Biosystems). qPCR gene expression was quantified relative to *Gapdh*. Primer sequences used were:

Mouse (5'-3'):

Epgn forward: TGGGGGTTCTGATAGCAGTC, *Epgn* reverse: GGATCACCTCTGCTTCTTCG, *Egf* forward: CCTGGGAATGTGATTGCTTT, *Egf* reverse: CCTGGGAATTTGCAAACAGT, *Hbegf* forward: CCACCTCACTCCCTTTGTGT, *Hbegf* reverse: AAAGCTCCCTGCTCTTCCTC, *Tgfa* forward: AAGGCATCTTGGGACAACAC, *Tgfa* reverse: GCAGGCAGCTTTATCACACA, *Btc* forward: GGGTGTTTCCCTGCTCTGTA, *Btc* reverse: TGGATGAGTCCTCAGGTTCC, *Areg* forward: CATTATGCAGCTGCTTTGGA, *Areg* reverse: TTTCGCTTATGGTGGAAACC, *Ereg* forward: CGCTGCTTTGTCTAGGTTCC, *Ereg* reverse: GGGATCGTCTTCCATCTGAA, *Adam17* forward: GATGCTGAAGATGACACTGTG, *Adam17* reverse: GAGTTGTCAGTGTCAACGC, *Gapdh* forward: ATGTGTCCGTCGTGGATCTGA, *Gapdh* reverse: TTGAAGTCGCAGGAGACAACCT.

Human (5’-3’):

Epgn forward: ATGACAGCACTGACCGAAGAG, *Epgn* reverse: AACTGTCCAGTTACCTTGCTG, *Egf* forward: TCTCAACCCCTTGTACTTTGG, *Egf* reverse: CAAGTCATCCTCCCATCACCA, *Hbegf* forward: TTGTGCTCAAGGAATCGGCT, *Hbegf* reverse: CAACTGGGGACGAAGGAGTC, *Tgfa* forward: TCGTGAGCCCTCGGTAAGTA, *Tgfa* reverse: GACTGGTCCCCCTTTCATGG, *Btc* forward: AAAGCGGAAAGGCCACTTCT, *Btc* reverse: AGCCTTCATCACAGACACAGG, *Areg* forward: TGTCGCTCTTGATATCGGC, A*reg* reverse: ATGGTTCACGCTTCCCAGAG, *Ereg* forward: TACTGCAGGTGTGAAGTGGG, *Ereg* reverse: GTGGAACCGACGACTGTGAT, *Adam17* forward: TGATGAGCCAGCCAGGAGAT, *Adam17* reverse: TATCAAGTCTTGTGGGGACAGC, *Gapdh* forward: CGACAGTCAGCCGCATCTT, *Gapdh* reverse: ATCCGTTGACTCCGACCTTC.

Skin histopathology scoring

A blinded expert dermatopathologist scored H&E stained sections based on dermal inflammation (0-3).

SUPPLEMENTARY FIGURES

Fig. S1

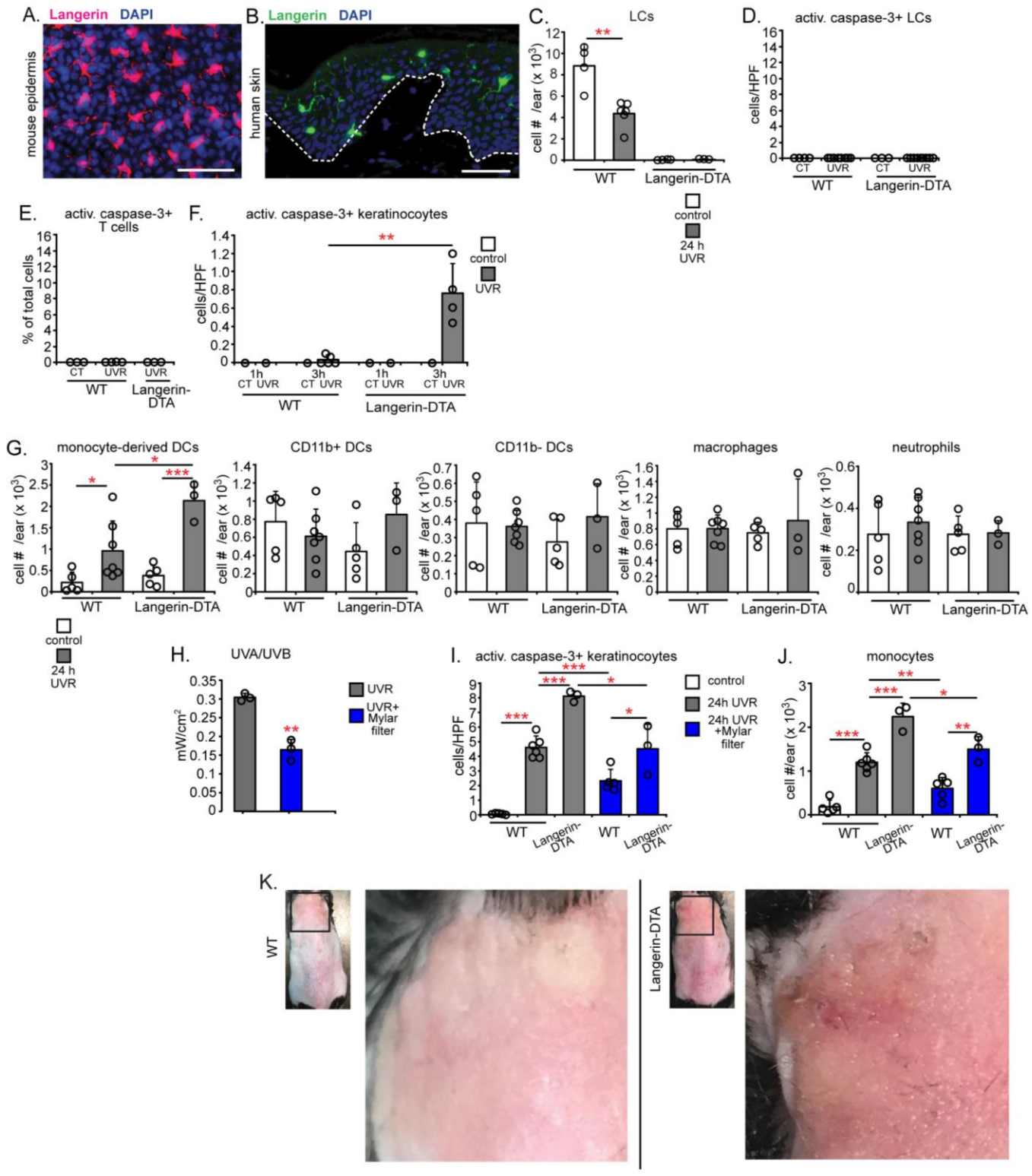

Fig. S1. Additional features of LC-mediated protection from UVR-induced keratinocyte apoptosis and skin injury. (A) Representative image of mouse epidermal whole mount

stained with anti-Langerin (pink) and DAPI (blue) (n= 3 mice). **(B)** Representative image of human skin stained with anti-Langerin (green) and DAPI (blue) (n= 3 healthy control human patients). Dashed line indicates epidermal-dermal junction. **(A,B)** Scale bar: 50 μm. **(C-E)** WT and Langerin-DTA mice were treated with UVR and ears examined at 24 hours as in Fig. 1A-C. **(C)** LC numbers as assessed by flow cytometry (n= 3-6 mice). **(D)** Activated caspase-3+ Langerin+ LC numbers in tissue sections (n= 3-9 mice). **(E)** Activated caspase-3+ CD3+ T cell numbers (n= 3-4 mice). **(F)** Activated caspase-3+ keratinocyte numbers at indicated time after UVR exposure (n= 1-4 mice). **(G)** Absolute numbers of monocyte-derived DCs, CD11b+ DCs, CD11b- DCs, macrophages, and neutrophils at 24 hours after UVR exposure (n= 3-7 mice). **(H)** UVA/UVB measurements of UVR source without and with Mylar filter (n= 3). Each symbol represents the value measured during independent experiments. **(I,J)** WT and Langerin-DTA mice were treated with UVR or UVR+Mylar filter and examined with non-exposed controls at 24 hours (n= 3-6 mice). **(I)** Activated caspase-3+ keratinocyte numbers. **(J)** Absolute monocyte numbers. **(K)** Magnified images of back skin from UVR-exposed WT and Langerin-DTA mice described in Fig. 1G,H (n= 3-5 mice). **(C-G,I-K)** Each symbol represents 1 mouse**.** Data from 3 **(A,B,E,H-K)**, 5 **(C)**, 9 **(D),** 2 **(F),** and 7 **(G)** independent experiments. Bars represent means and error bars depict standard deviations. *****$p<0.05$, **$p<0.01$, ***$p<0.001$ using two-tailed unpaired Student's t-test. T-test was performed after one-way ANOVA for **(C-G, I, J)**.

Fig. S2

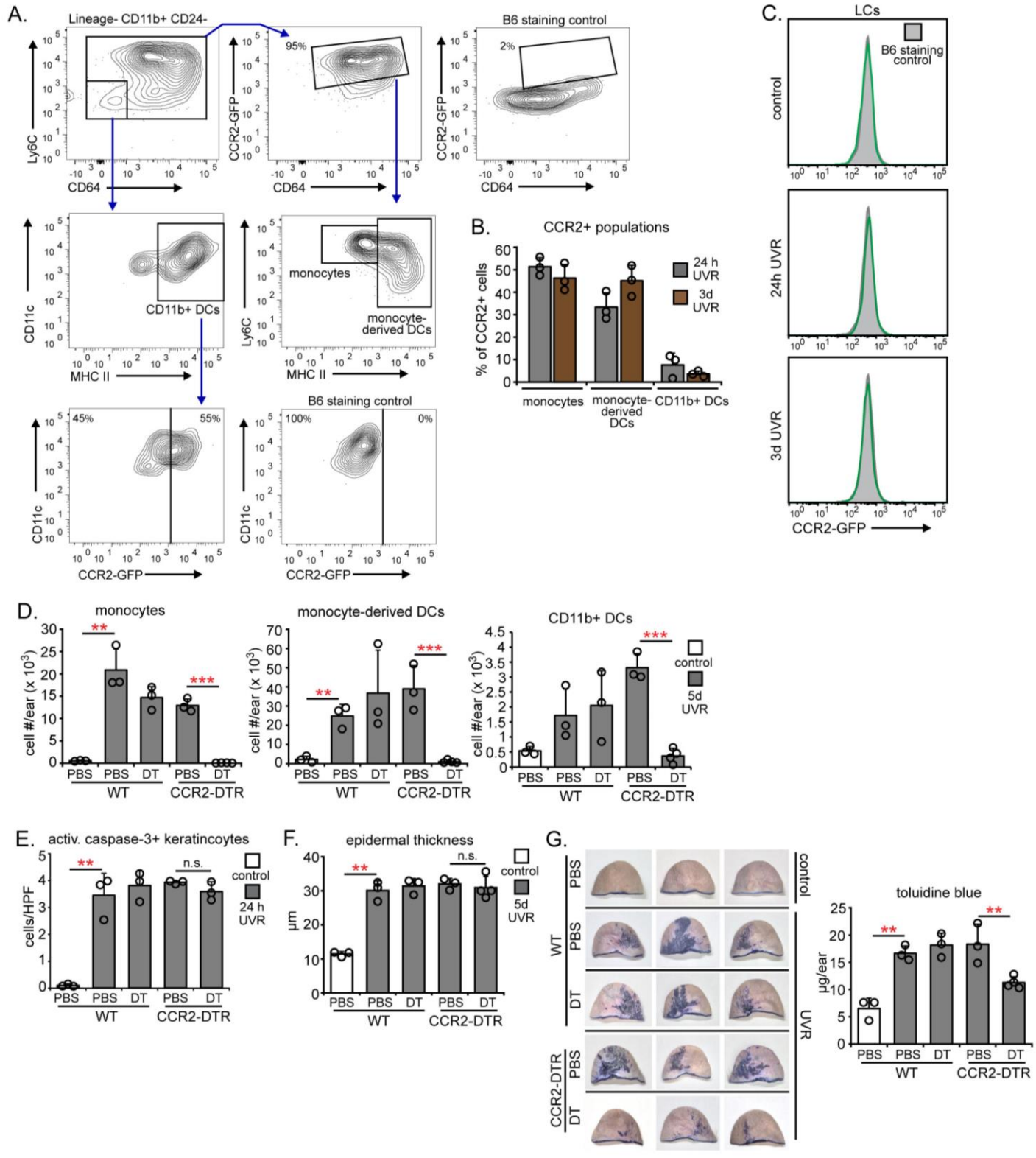

Fig. S2. The role of accumulated monocytes and monocyte-derived DCs in UVR-induced skin injury. **(A-C)** CCR2-GFP reporter mice were exposed to UVR and ears were examined at

indicated time points along with a B6 staining control (n= 3 mice). **(A)** Flow cytometry gating strategy for CCR2+ populations in the skin using the scheme of Tamoutounour et. al (*24*). Lineage= B220, CD3, Ly6G, and pan-NK CD49b **(B)** Percentage of CCR2+ cells in the skin that are monocytes, monocyte-derived DCs, and CD11b+ DCs. **(C)** Representative histograms of CCR2-GFP expression in LCs as assessed by flow cytometry (n= 3 mice). **(D-G)** WT and CCR2-DTR mice were injected with PBS or 250 ng DT at d-1 and d0 of UVR exposure and examined 24 hours later with non-exposed control mice (n= 3 mice) **(E),** or injected with PBS or DT at d-1, d0, and d3 of UVR exposure and examined 5 days later with non-exposed control mice (n= 3-4 mice) **(D,F,G)**. **(D)** Monocyte, monocyte-derived DC, and CD11b+ DC depletion at 5 days after UVR exposure. **(E)** Activated caspase-3+ keratinocyte numbers. **(F)** Epidermal thickness. **(G)** Epidermal permeability. Left: Representative images of toluidine blue penetrance. Right: Quantification. **(B,D-G)** Each symbol represents 1 mouse**.** Data from 2 **(A-C,E)** and 3 **(D,F,G)** independent experiments. Bars represent means and error bars depict standard deviations. n.s.= not significant $p \geq 0.05$,**$p<0.01$, ***$p<0.001$ using two-tailed unpaired Student's t-test after one-way ANOVA.

Fig. S3

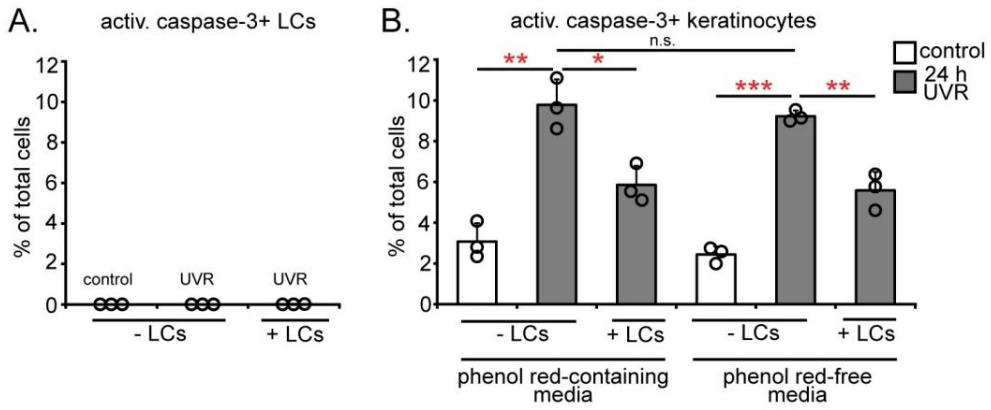

Fig. S3. Additional features of LC-mediated protection of keratinocytes in vitro. (A) Murine keratinocyte cultures without and with LCs were exposed to UVR (as in Fig. 2D,E) and activated caspase-3+ cells that were Langerin+ (LCs) were quantified (n= 3 mice). **(B)** LC-mediated protection of keratinocytes in the absence of phenol red. Murine keratinocyte cultures without and with LCs were exposed to UVR in phenol red-containing media (used for most experiments) or phenol red-free keratinocyte growth media and activated caspase-3+ keratinocyte numbers were quantified (n= 3 mice). Results are from 3 **(A)** and 2 **(B)** independent experiments, with each symbol representing a biological replicate. Each biological replicate value is the mean obtained from 2-6 replicate wells. n.s.= not significant $p \geq 0.05$, ***p<0.05, **p<0.01, ***p<0.001 using two-tailed unpaired Student's t-test after one-way ANOVA.

Fig. S4

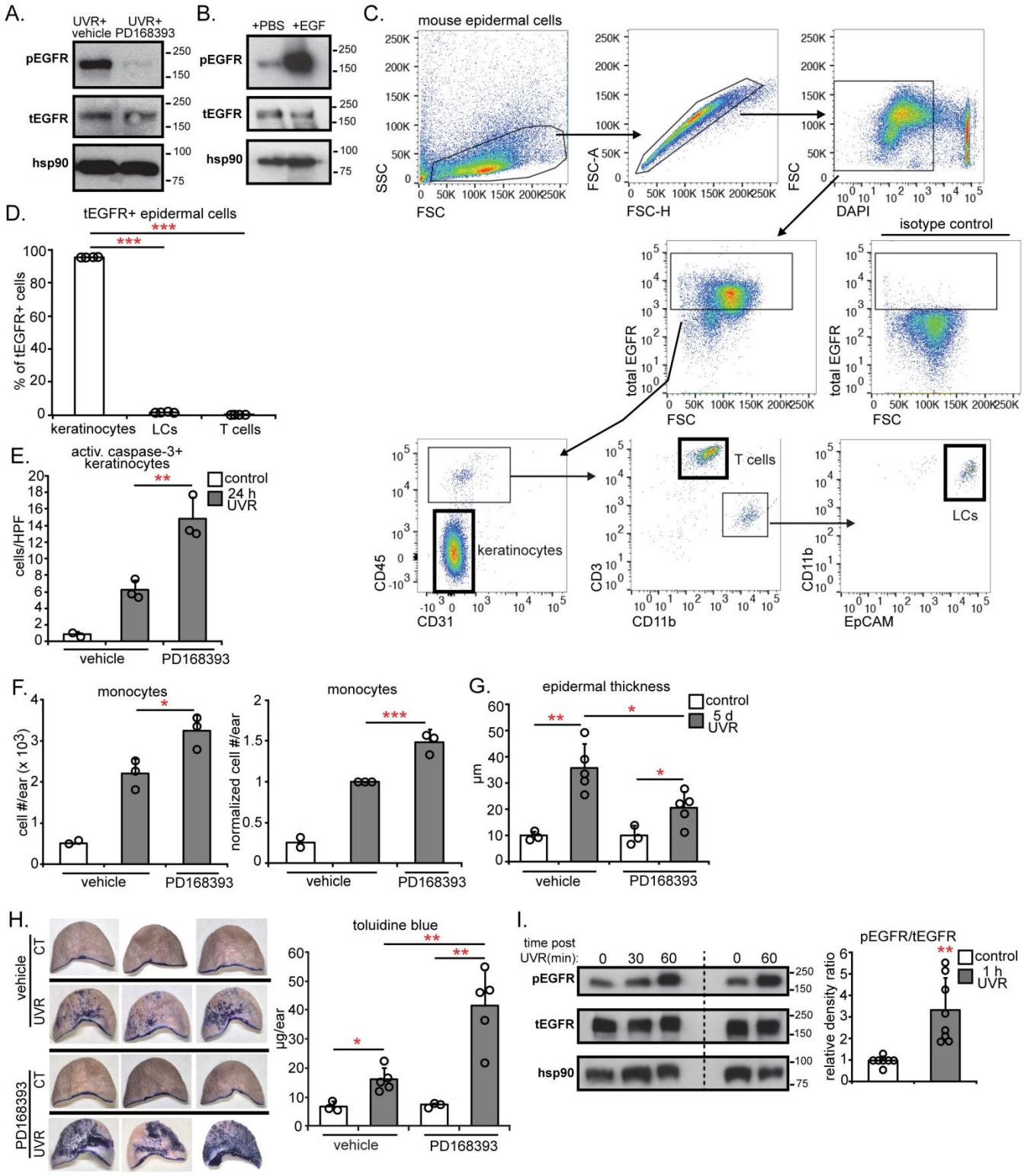

Fig. S4. Mice treated with EGFR inhibitor resemble Langerin-DTA mice and timing of epidermal EGFR activation after UVR exposure. (A, E-H) Mice were treated topically with 4mM EGFR inhibitor-PD168393 or vehicle prior to UVR exposure and examined at indicated

time points. **(A)** Representative Western blot of epidermal EGFR phosphorylation at 1 hour after UVR (n= 3 mice). **(B)** Positive control for EGFR phosphorylation, showing effects of intradermally injected recombinant EGF (5µg) at 5 minutes (n= 2 mice). **(C)** Flow cytometry gating strategy for total EGFR (tEGFR)+ cells in the epidermis. **(D)** Percent of tEGFR+ cells in each epidermal cell population examined (n= 4 mice). **(E)** Activated caspase-3+ keratinocyte numbers (n= 2-3 mice). **(F)** Absolute (left) and normalized (right) monocyte numbers (n= 2-3 mice) **(G)** Epidermal thickness (n= 3-5 mice). **(H)** Epidermal permeability. Representative images of toluidine blue-treated ears (left) and quantification (right) (n= 3-5 mice). **(I)** Left: Representative Western blot at the indicated time points after UVR exposure. Right: phosphoEGFR:total EGFR relative density ratio (n= 7-8 mice). **(D-I)** Each symbol represents 1 mouse**.** Data from 3 **(A,E,F)**, 1 **(B,D)**, 2 **(G,H)**, and 4 **(I)** independent experiments. Bars represent means and error bars depict standard deviations. *****p<0.05, **p<0.01, ***p<0.001 using two-tailed unpaired Student's t-test. T-test was performed after one-way ANOVA for **(D-H)**.

Fig. S5

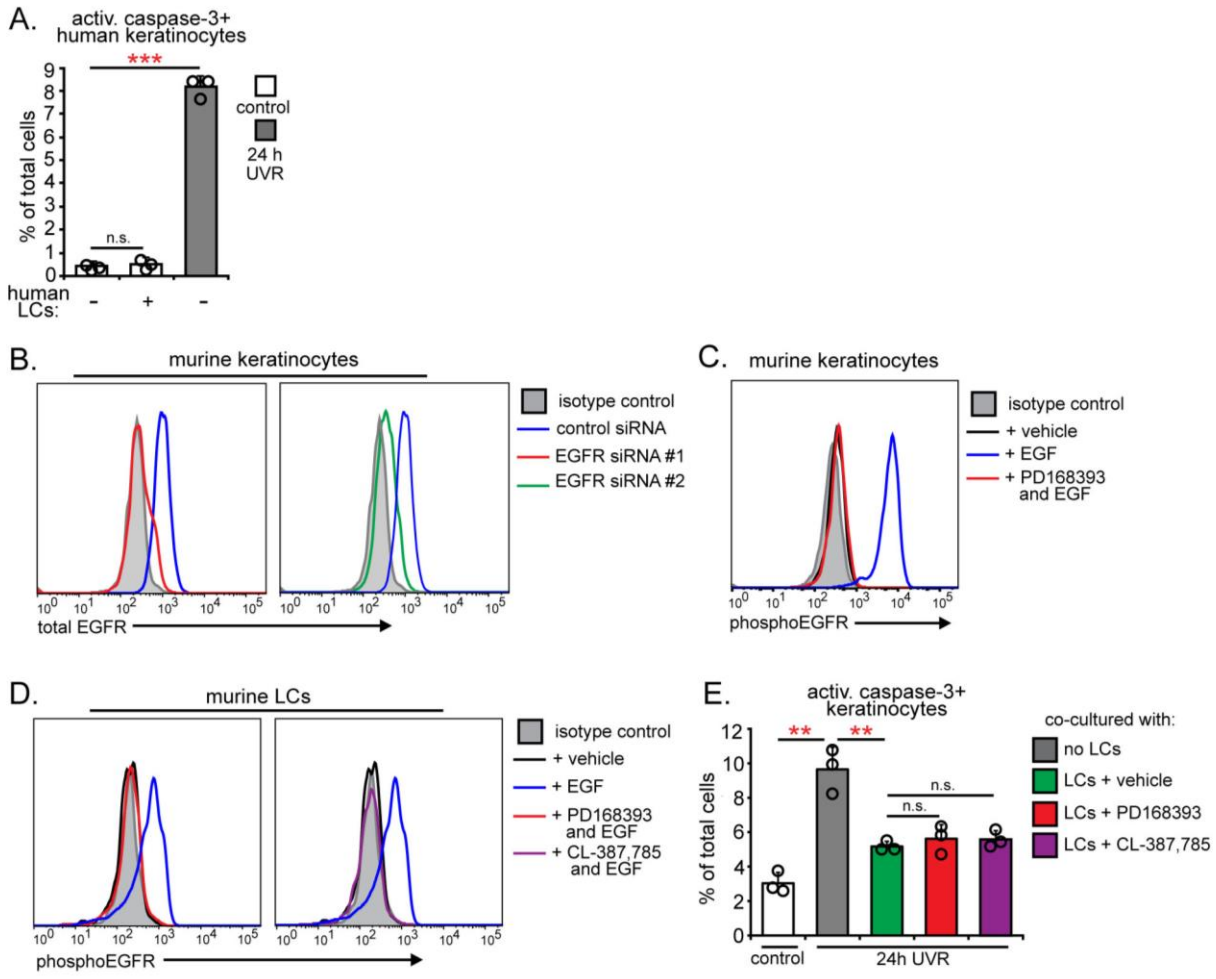

Fig. S5. Effect of human LCs on human keratinocytes without UVR and further characterization of in vitro LC-keratinocyte EGFR signaling (A) Effect of human LCs on human keratinocytes without UVR. Primary human keratinocytes were co-cultured with or without human LCs and activated caspase-3+ keratinocytes were enumerated 24 hours later (n= 3 human LC donors). **(B)** Validation of siRNA-mediated EGFR knockdown in primary murine keratinocytes. Keratinocytes were treated with control or EGFR-targeted siRNAs (#1 and #2) and EGFR expression was measured 5 days later (on the day of UVR exposure as in Fig. 3F) by flow cytometry. Representative histogram of EGFR expression in keratinocytes. (n= 4 mice). **(C)** Validation of pharmacological EGFR inhibition in primary murine keratinocytes.

EGF-starved primary murine keratinocytes were pre-treated with vehicle or 2 μM PD168393 for 30 minutes, then treated with EGF (200 ng/mL) for 10 minutes, and phosphoEGFR was then measured by flow cytometry. Representative histogram of phosphoEGFR expression in keratinocytes (n= 3 mice). **(D)** Validation of pharmacological EGFR inhibition in LCs. LCs were sorted from WT mice, serum-starved, pre-treated with vehicle, 2 μM PD168393, or an alternate EGFR inhibitor, CL-387,785 (1 μM) for 30 minutes, then treated with EGF (200 ng/mL) for 10 minutes, and phosphoEGFR measured by flow cytometry. Representative histogram of phosphoEGFR expression in LCs (n= 3 mice). **(E)** Effect of LC EGFR inhibition on LC-mediated protection of keratinocytes. Murine keratinocyte cultures without and with the indicated pre-treated LCs were exposed to UVR and activated caspase-3+ keratinocytes were enumerated 24 hours later (n= 3 mice). Results are from 4 **(B)**, 2 **(C,E)**, and 3 **(A,D)** independent experiments. **(A,D)** Each symbol represents a biological replicate and each biological replicate value is the mean obtained from 2-3 replicate wells. Bars represent means and error bars depict standard deviations. n.s.= not significant $p \geq 0.05$, $^{**}p < 0.01$ using two-tailed unpaired Student's t-test after one-way ANOVA.

Fig. S6

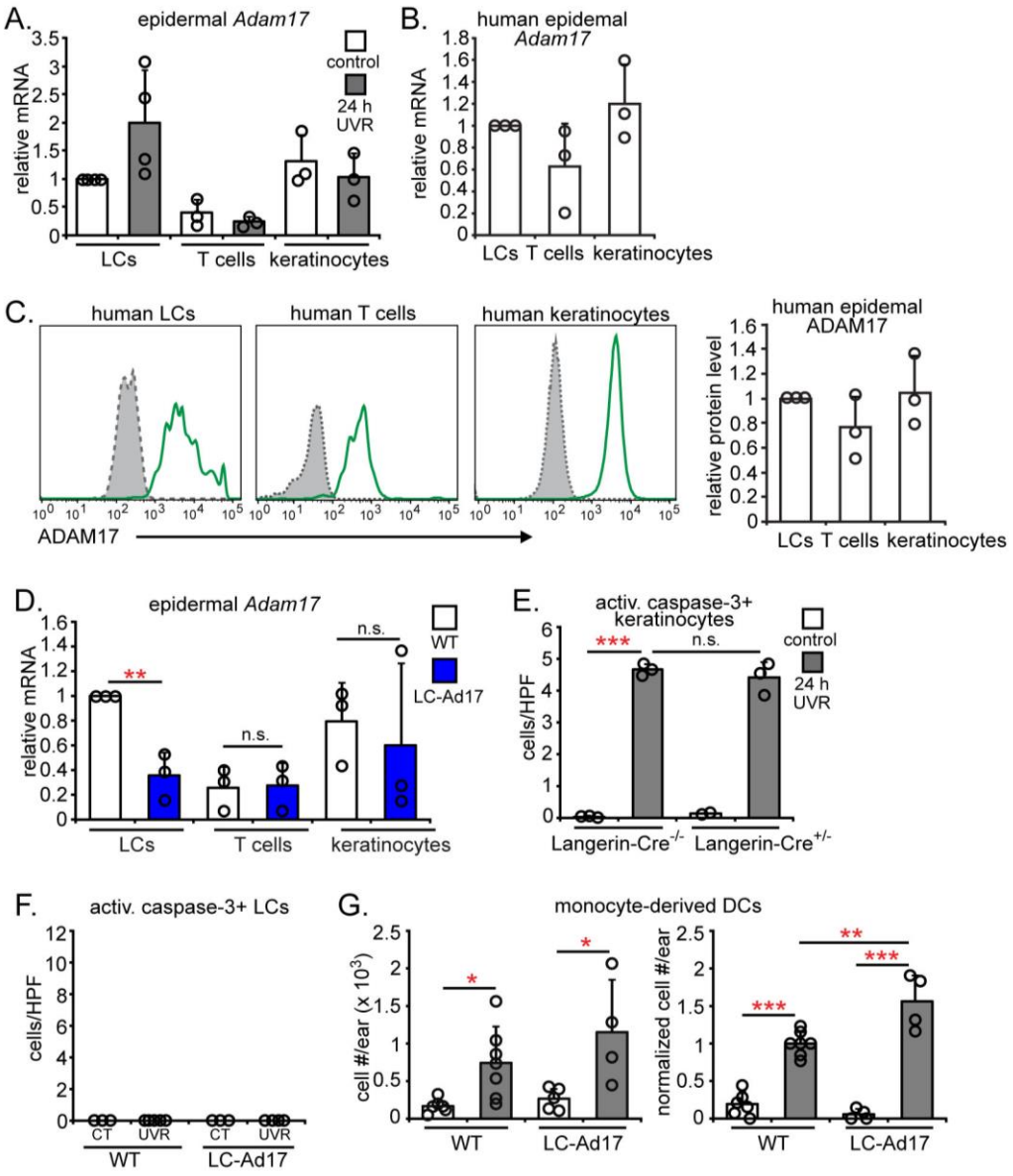

Fig. S6. Characterization of mouse and human ADAM17 expression, LC-Ad17 mice, and Langerin-Cre mice (A) *Adam17* expression in epidermal cell subsets sorted from non-exposed WT mice or from mice at 24 hours after UVR exposure, normalized to control LC expression (n= 3-4 mice). **(B)** *Adam17* mRNA expression in sorted LCs, T cells, and keratinocytes from healthy human skin, normalized to LC expression (n= 3 human donors). **(C)** ADAM17 cell surface protein expression on human LCs, T cells, and keratinocytes as assessed by flow cytometry (n= 3 human donors). Top: Representative histograms. Bottom:

Quantification of relative ADAM17 protein levels. MFI of ADAM17 stain was first divided by MFI of isotype control to quantify fold-over-isotype for each cell type and the fold-over-isotype for each cell type was then expressed relative to that of LC ADAM17. **(D)** *Adam17* expression in epidermal cell subsets sorted from WT and LC-Ad17 mice at homeostasis normalized to WT LC expression (n= 3 mice). **(E)** Langerin-Cre$^{-/-}$ and Langerin-Cre$^{+/-}$ mice were exposed to UVR and activated caspase-3+ keratinocytes quantified (n= 2-3 mice). **(F)** Activated caspase-3+ LC numbers in WT and LC-Ad17 mice (n= 3-5 mice). Data are from same mice as in Fig. 5A. **(G)** Absolute (left) and normalized (right) monocyte-derived DC numbers in WT and LC-Ad17 mice (n= 4-7 mice). **(A-G)** Each symbol represents 1 mouse or 1 human donor. Data from 4 **(A)**, 3 **(B-F)**, or 5 **(G)** independent experiments. Bars represent means and error bars depict standard deviations. n.s.= not significant $p \geq 0.05$, *****$p<0.05$, **$p<0.01$, ***$p<0.001$ using two-tailed unpaired Student's t-test after one-way ANOVA.

Fig. S7

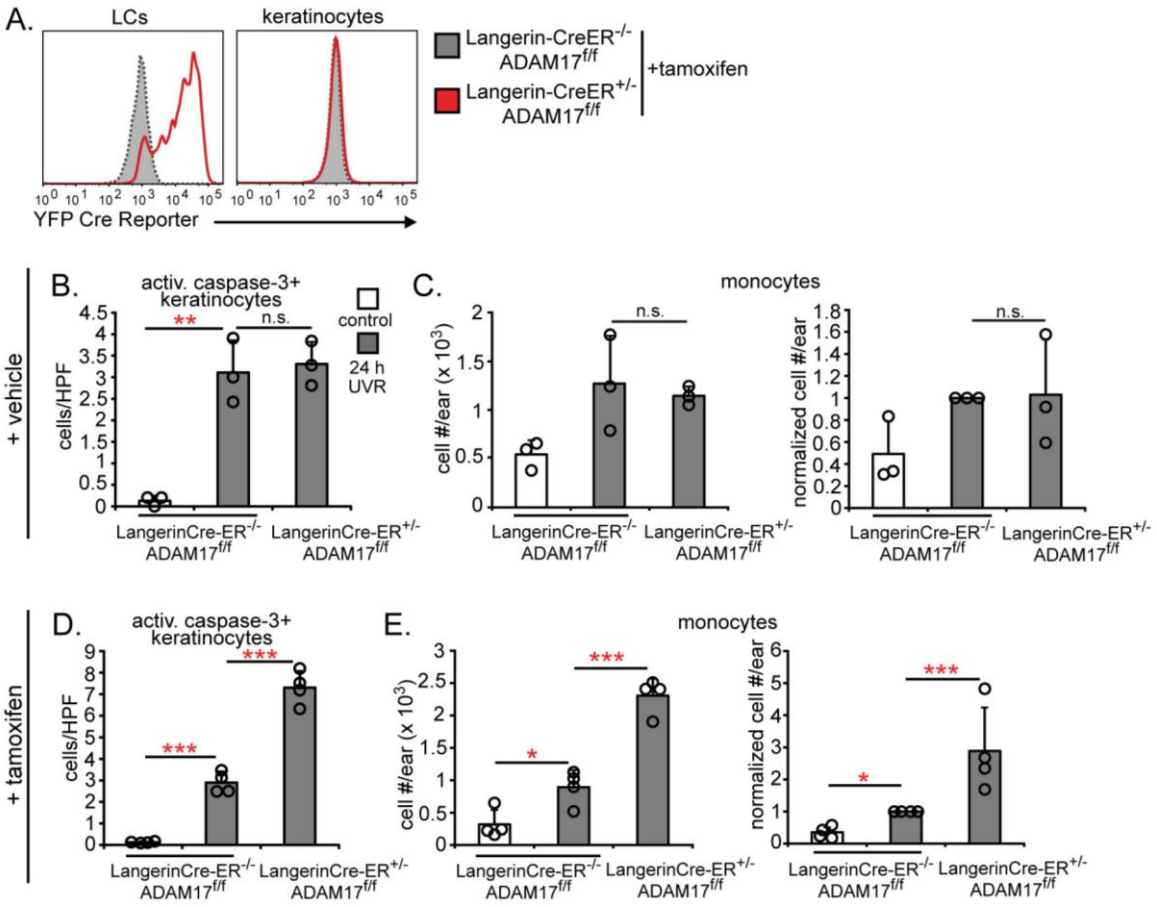

Fig. S7. Effects of inducible ADAM17 deletion in LCs. (A-E) Langerin-Cre-ER$^{-/-}$ ADAM17$^{flox/flox}$ and Langerin-Cre-ER$^{+/-}$ADAM17$^{flox/flox}$ mice containing a Rosa26.STOP^{fl}.YFP Cre reporter allele were generated and treated topically with vehicle (n= 3 mice) **(B,C)** or 1 ng/mL 4-hydroxytamoxifen (n= 4 mice) **(A,D,E)**. Six days later, they were either examined **(A)** or exposed to UVR and analyzed at 24 hours **(B-E).** **(A)** Cre expression in LCs. Shown is representative histogram of YFP levels in LCs and keratinocytes. **(B,D)** Activated caspase-3+ keratinocyte numbers. **(C,E)** Absolute (left) and normalized (right) monocyte numbers. **(B-E)** Each symbol represents 1 mouse. Data from 2 (A,D,E) and 1 (B,C) independent experiments. Bars represent means and error bars depict standard deviations. n.s.= not significant $p \geq 0.05$, ***p<0.05, **p<0.01, ***p<0.001 using two-tailed unpaired Student's t-test after one-way ANOVA.

Fig. S8

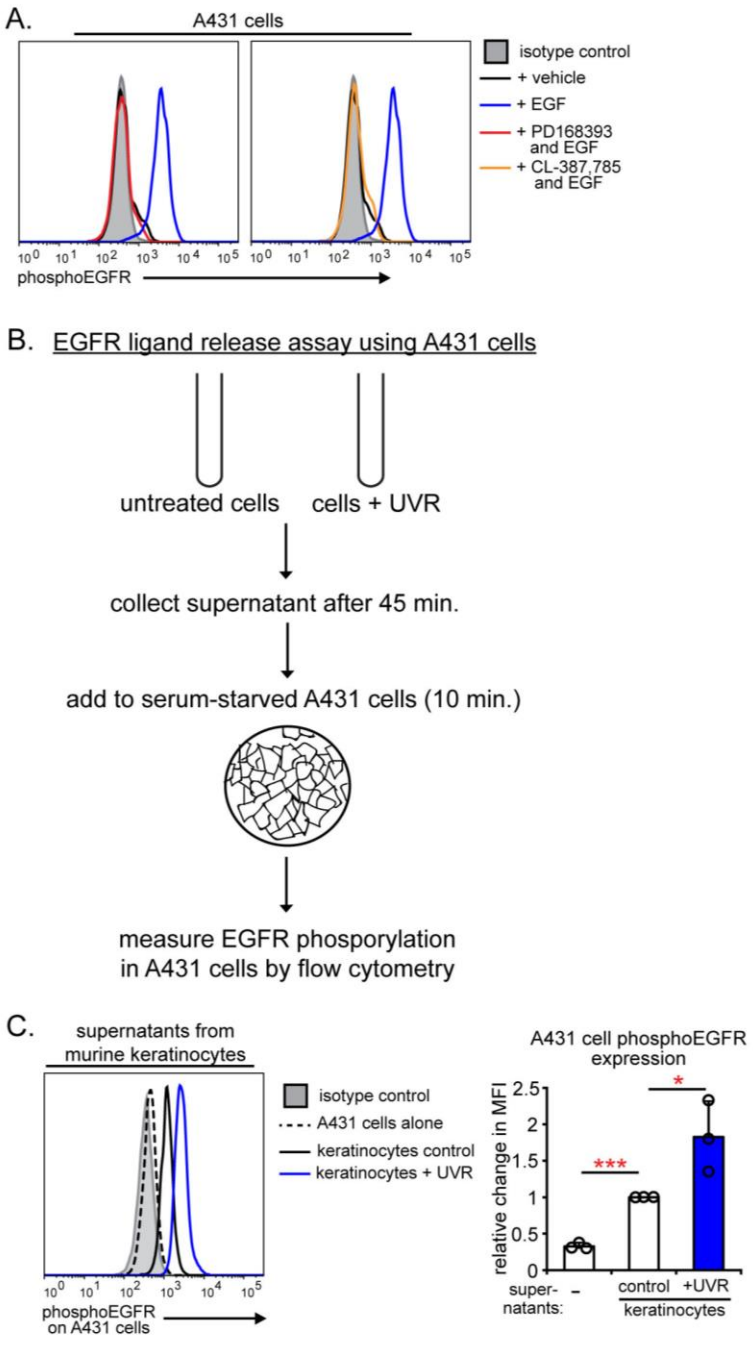

Fig. S8. Validation of EGFR ligand release assay and characterization of keratinocyte EGFR ligand release. (A) A431 indicator cells were serum-starved overnight then pre-treated for 15 minutes with vehicle, the irreversible EGFR inhibitors PD168393 (2 μM), or CL-387,785 (1 μM). The cells were then treated with EGF (100 ng/mL) for 10 minutes and phosphoEGFR

was measured by flow cytometry (n= 2 separate cell passages). **(B)** Schematic diagram of EGFR ligand release assay using A431 indicator cells. Cells (sorted murine LCs, sorted human LCs, or primary murine keratinocytes) were treated or not with UVR and the conditioned supernatant was collected and added to serum-starved A431 cells for 10 minutes. The A431 cells were then collected and phosphoEGFR was measured by flow cytometry as an indicator of the level of EGFR ligand in the conditioned supernatant. **(C)** Characterization of murine primary keratinocyte EGFR ligand release. Confluent primary murine keratinocytes were exposed to UVR and the supernatant of these cells and non-exposed control keratinocytes was collected 45 minutes later and added to A431 cells as described in Fig. S7B. Left: Representative histogram of phosphoEGFR expression in the A431 cells. Right: Quantification of A431 cell phosphoEGFR expression normalized to the expression with control keratinocyte supernatants (n= 3 mice). Results are from 2 **(A,C)** independent experiments. **(C)** Each symbol represents a biological replicate. Bars represent means and error bars depict standard deviations. ***$p<0.001$, *$p<0.05$ using two-tailed unpaired Student's t-test after one-way ANOVA.

Fig. S9

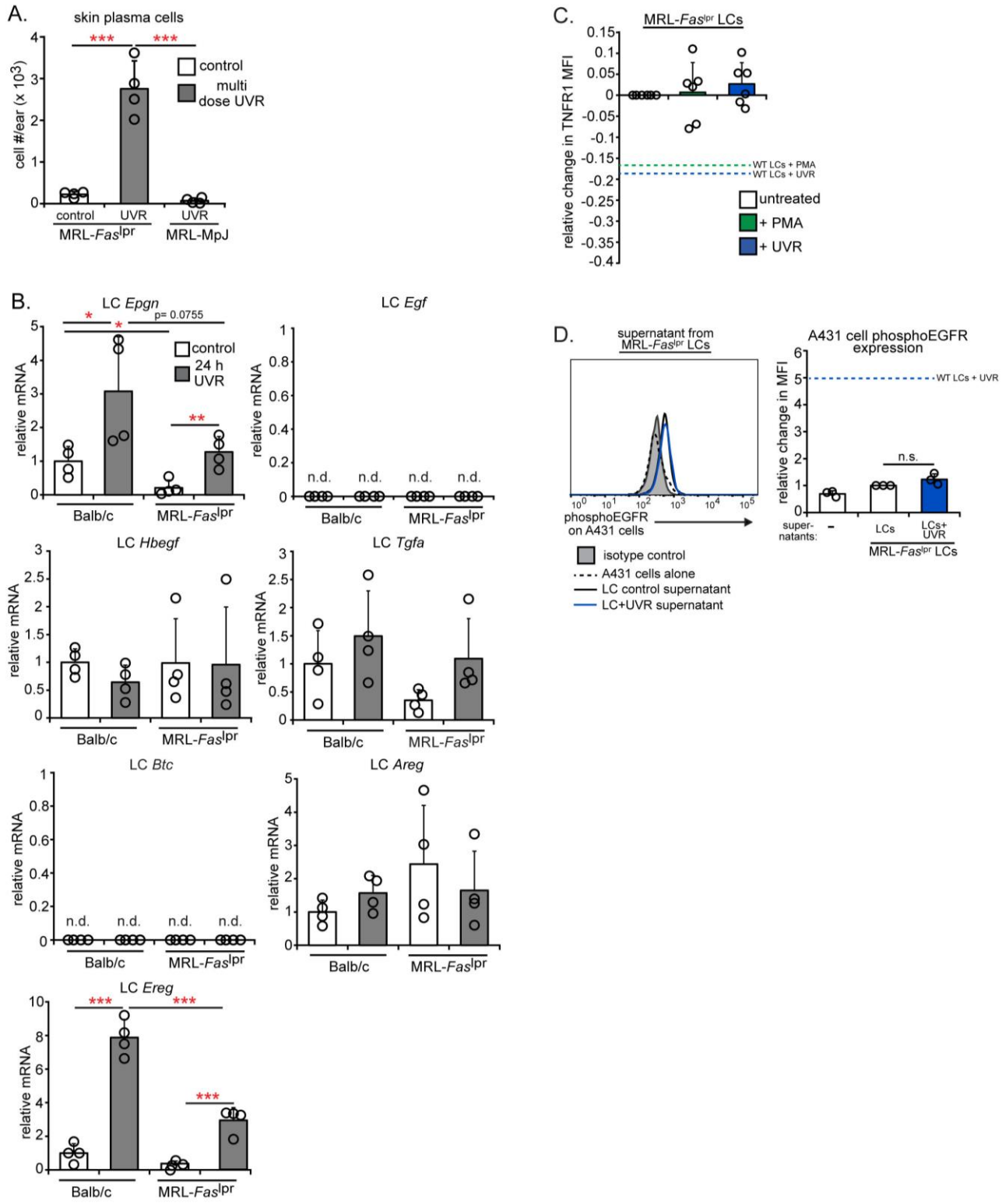

Fig. S9. Photosensitive MRL-*Fas*^{lpr} mice have more skin plasma cells and reduced LC EGFR ligand expression, LC ADAM17 activity, and LC EGFR ligand release. (A,B) MRL-

Fas^{lpr} and non-lupus MRL-MpJ or Balb/c mice were exposed to UVR as indicated and skin from these and non-exposed control mice were examined 24 hours after the final exposure (n= 4 mice). **(A)** Skin plasma cells (CD45+, B220^{lo}, CD3-, intracellular IgG^{hi}) after 6 days of UVR exposure. **(B)** Mice were exposed to a single UVR dose and LCs were sorted from these and control mice 24 hours later. LC expression of EGFR ligands normalized to that of control Balb/c mice. **(C)** MRL-*Fas*^{lpr} LC ADAM17 activity. LCs sorted from MRL-*Fas*^{lpr} mice were treated with PMA or UVR and the percent change in TNFR1 MFI relative to that of untreated LCs was measured 45 minutes later by flow cytometry (n= 6 mice). Dashed lines indicate the relative change in TNFR1 MFI observed in WT mice treated with PMA (green) or UVR (blue) as in Fig. 5A. **(D)** Conditioned supernatants from untreated and UVR-exposed MRL-*Fas*^{lpr} LCs were added to A431 EGFR indicator cells and phosphoEGFR in the A431 cells was measured 10 minutes later by flow cytometry (n= 3 mice). Dashed line indicates the relative change in phosphoEGFR MFI observed with UVR-exposed WT LC supernatants as in Fig. 5C. **(A,B)** Each symbol represents 1 mouse. **(C,D)** Each symbol represents a biological replicate, which is the average of 1-4 replicate wells. Data from 3 **(A,D),** 2 **(B),** and 6 **(C)** independent experiments. Bars represent means and error bars depict standard deviations. n.s.= not significant $p \geq 0.05$, *****$p<0.05$, **$p<0.01$, ***$p<0.001$ using two-tailed unpaired Student's t-test after one-way ANOVA.

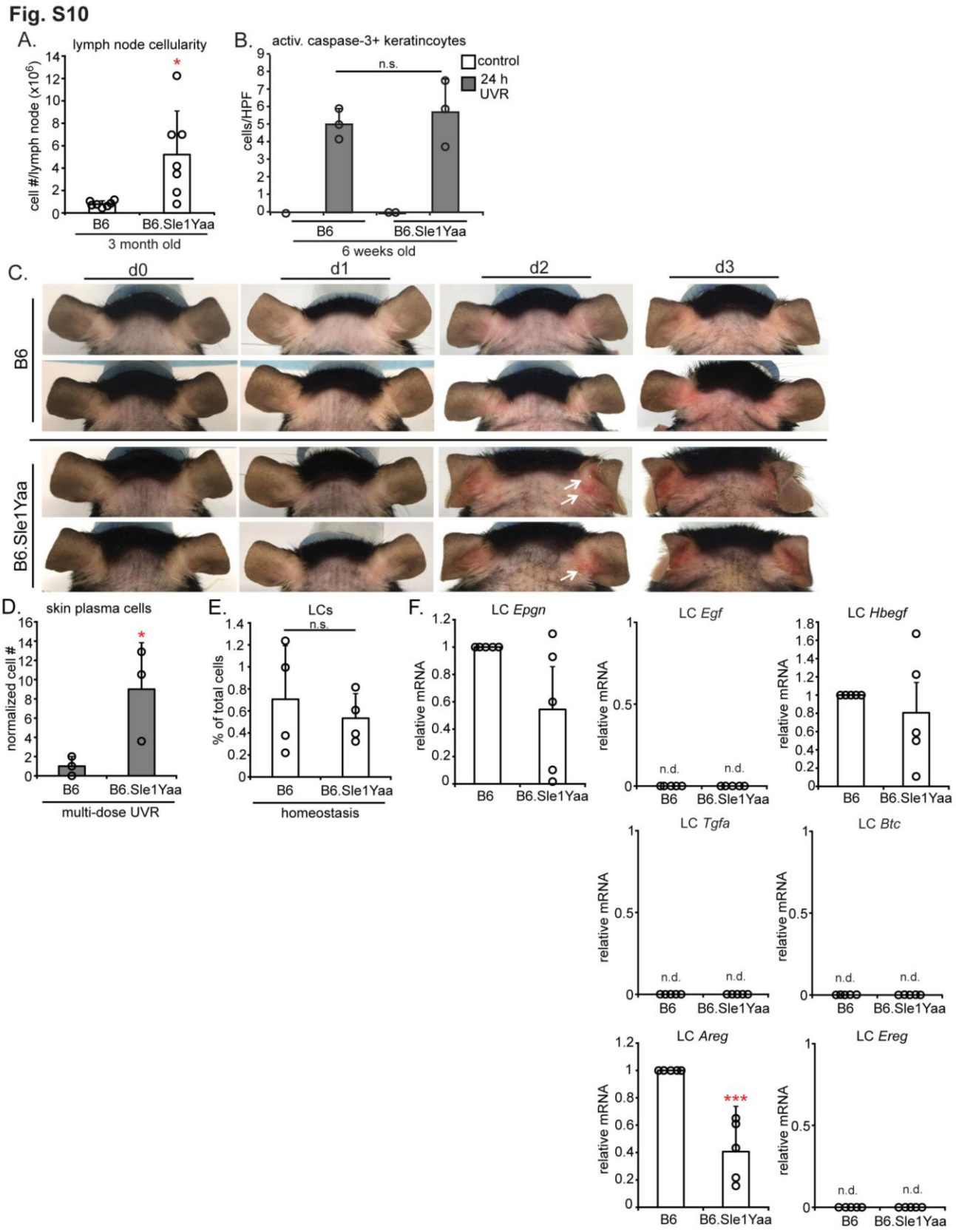

Fig. S10. B6.Sle1yaa mice exhibit photosensitivity and characterization of EGFR ligand expression by their LCs. (A) Popliteal lymph node cellularity at 3 months of age (n= 7 mice).

(B) Activated caspase-3+ keratinocyte numbers in 6 week old B6.Sle1yaa mice or age-matched B6 mice (n= 2-3 mice). **(C,D)** 8-12 month old B6.Sle1yaa mice and age-matched B6 mice were exposed to UVR for 6 days starting at day 0 (d0) and ears harvested 24 hours after the final exposure (n= 3 mice). **(C)** Images of representative ears at the indicated time points of UVR exposure. White arrows indicate visible lesions. **(D)** Normalized number of plasma cells in the skin as measured by flow cytometry. **(E,F)** 8-12 month old B6.Sle1yaa mice or age-matched B6 mice were examined at homeostasis. **(E)** Percent of LCs in skin as measured by flow cytometry (n= 4 mice). **(F)** B6.Sle1yaa LC expression of EGFR ligands. LCs were sorted from homeostatic B6 and B6.Sle1yaa mice and mRNA expression was normalized to that of B6 mice (n= 5 mice). n.d.= not detectable. **(A,B,D-F)** Each symbol represents 1 mouse**.** Data from 7 **(A)**, 3 **(B)**, 2 **(C,D)**, 4 **(E)**, and 5 **(F)** independent experiments. Bars represent means; error bars depict standard deviations. n.s.= not significant $p \geq 0.05$, ***** $p < 0.05$, *** $p < 0.001$ using two-tailed unpaired Student's t-test. T-test was performed after one-way ANOVA for **(B)**.

Fig. S11

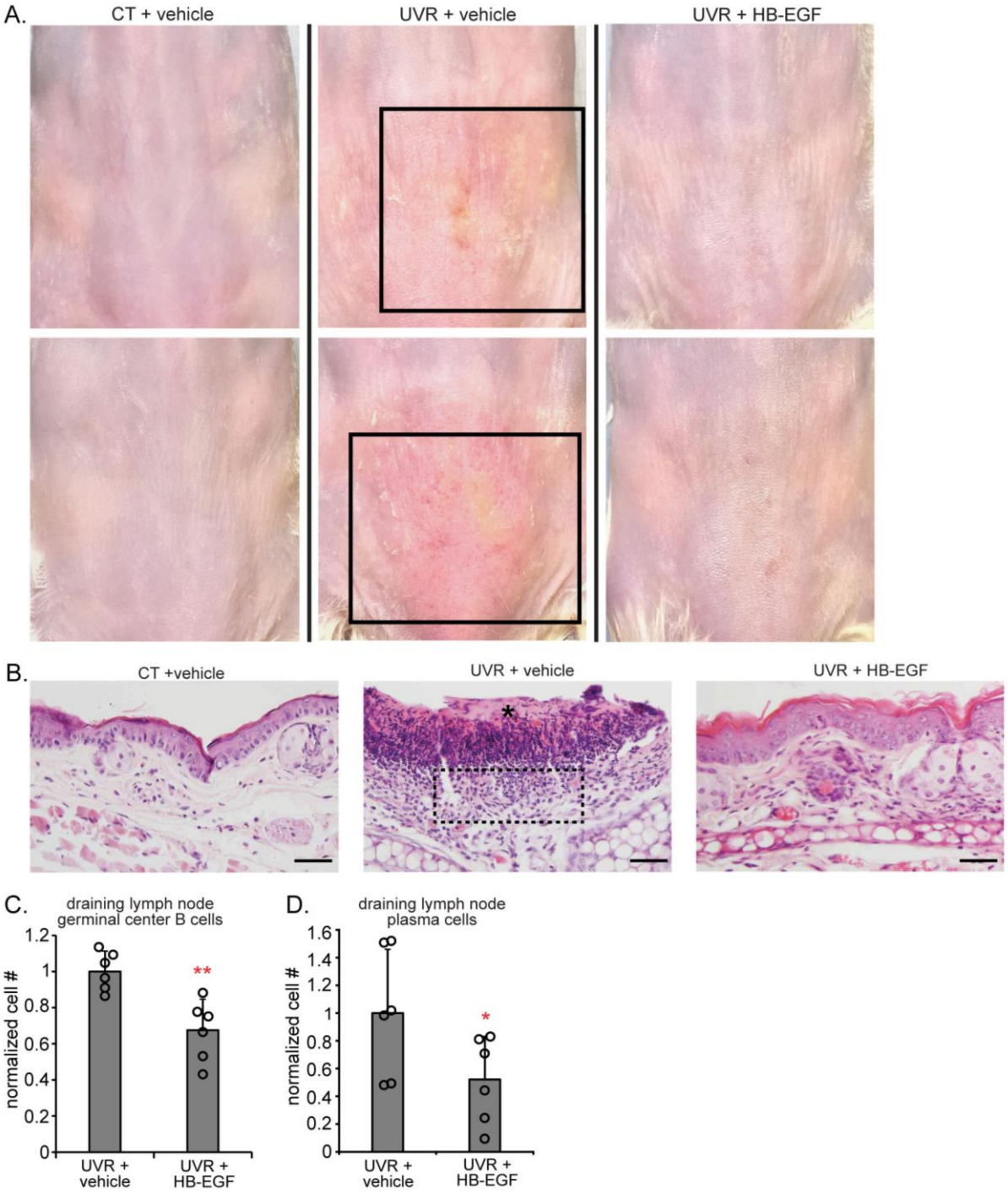

Fig. S11. EGFR ligand application reduces the severity of UVR-induced skin lesions and lymph node B cell responses in SLE model mice. (A-C) Mice were treated with HB-EGF as in Fig. 8A-E (n= 4 mice). **(A)** Magnified images of back lesions as shown in Fig. 8C. Boxes

outline lesional areas. **(B)** Representative H&E images of ear skin. Neutrophil-dominant infiltrate (dashed box); ulceration (*). Scale bar: 50 μm. **(C,D)** Germinal center B cell **(C)** and plasma cell **(D) numbers** in skin draining lymph nodes (auricular and inguinal) normalized to mice treated with UVR+vehicle. **(C,D)** Each symbol represents either inguinal or auricular lymph nodes from multiple mice. Data from 3 **(A,B)** and 2 **(C,D)** independent experiments. Bars represent means. Error bars depict standard deviations. *****$p<0.05$ and **$p<0.01$ using two-tailed unpaired Student's t-test.

Fig. S12

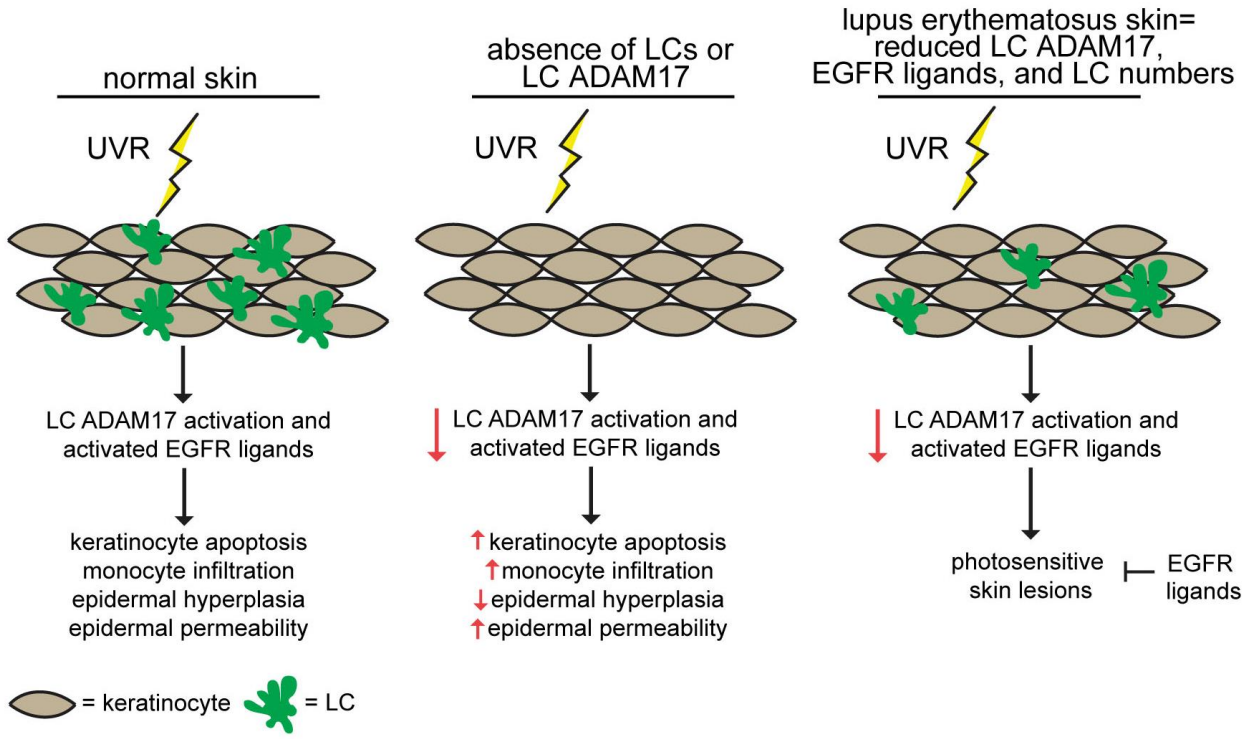

Fig S12. Model of protective LC-keratinocyte axis and dysfunction of this axis in lupus photosensitivity. In normal skin, LCs express ADAM17 and EGFR ligands. UVR stimulates LC ADAM17 activity and LCs provide activated EGFR ligands and limit the extent of keratinocyte apoptosis and skin injury. In the absence of LCs or with ADAM17 deletion in LCs, UVR-induced keratinocyte apoptosis and skin injury are increased. In lupus erythematosus, LCs are less able to provide activated EGFR ligands to keratinocytes, because of reduced ADAM17, reduced EGFR ligand expression, and/or reduced LCs, leading to photosensitivity. The provision of EGFR ligands could be a useful therapeutic approach for photosensitivity.

Fig. S13

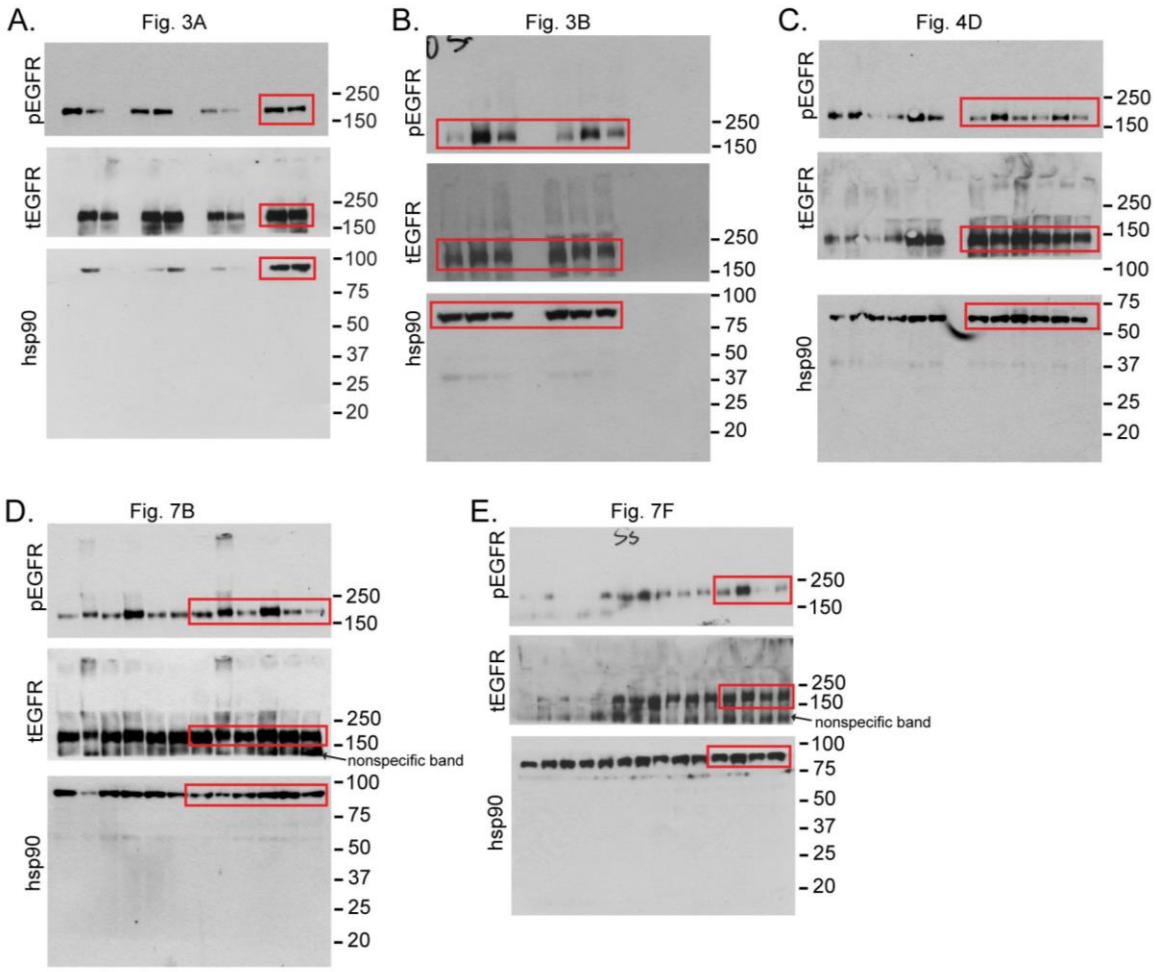

Fig. S13. Uncropped Western blot images. Uncropped Western blot from Fig. 3A **(A)**, Fig. 3B **(B)**, Fig. 4D **(C)**, Fig. 7B **(D)**, and Fig. 7F **(E)**. Western blots were stained with anti-phosphoEGFR (175 kDa) and anti-hsp90 (90 kDa), then stripped and stained with anti-total EGFR (175 kDa). Red boxes indicate the portion of the blots that are included in the main figure and arrows indicate non-specific bands.

Antibody (Clone)	Supplier	Catalog #	Lot #	Used for	Validation
Armenian hamster anti-mouse CD3 biotin (145-2C11)	BioLegend	100304	B216147	FC,IF	By manufacturer
rat anti-mouse Ly6G biotin (1A8)	BioLegend	127604	B218529	FC	By manufacturer
rat anti-mouse B220 biotin (RA3-6B2)	BioLegend	103204	B191786	FC	By manufacturer
rat anti-mouse CD49b biotin (DX5)	eBiosciences	13-5971-81	4295252	FC	By manufacturer
rat anti-mouse CD45 AlexaFlour700 (30-F11)	BioLegend	103128	B211311	FC	By manufacturer
rat anti-mouse CD45 PerCPCy5.5 (30-F11)	BioLegend	103132	B218549	FC	By manufacturer
Armenian hamster CD11c APCCy7 (N418)	BioLegend	117324	B237079	FC	By manufacturer
mouse anti-mouse Iab PE (AF6-120.1)	BioLegend	116408	B177711	FC	By manufacturer
mouse anti-mouse Iab FITC (AF6-120.1)	BDBiosciences	553551	62094	FC	By manufacturer
rat anti-mouse CD24 PerCPCy5.5	BioLegend	101824	B195555	FC	By manufacturer
rat anti-mouse CD11b Brillant Violet 570 (M1/70)	BioLegend	101233	B236974	FC	By manufacturer
rat anti-mouse CD11b PE (M1/70)	BioLegend	101208	B228654	FC	By manufacturer
rat anti-mouse CD11b FITC (M1/70)	BioLegend	101206	B192968	FC	By manufacturer
rat anti-mouse CD3 APCCy7 (145-2C11)	BioLegend	100330	B190252	FC	By manufacturer
rat anti-mouse CD3 FITC (145-2C11)	BDBiosciences	553062	5166876	FC	By manufacturer
rat anti-mouse Ly6C PECy7 (HK1.4)	BioLegend	128018	B242951	FC	By manufacturer
rat anti-mouse Ly6C FITC (HK1.4)	BioLegend	128006	B180475	FC	By manufacturer
mouse anti-mouse CD64 APC (X54-5/7.1)	BioLegend	139306	B207411	FC	By manufacturer
mouse anti-mouse CD64 PE (X54-5/7.1)	BioLegend	139304	B171679	FC	By manufacturer
rat anti-mouse CD31 PerCPCy5.5 (390)	BioLegend	102420	B219868	FC	By manufacturer
rat anti-mouse EpCAM PECy7 (G8.8)	BioLegend	118216	B176413	FC	By manufacturer
rat anti-mouse EpCAM APC (G8.8)	BioLegend	118214	B173069	FC	By manufacturer
rat anti-mouse Sca-1 APCCy7 (D7)	BioLegend	108126	B214144	FC	By manufacturer

rat anti-mouse CD49f biotin (GoH3)	BioLegend	313604	B226568	FC	By manufacturer
Armenian hamster anti-mouse CD103 PE (2E7)	BioLegend	121406	B184715	FC	By manufacturer
Armenian hamster anti-mouse CD103 APC (2E7)	BioLegend	121413	B222546	FC	By manufacturer
Armenian hamster TNFR1/p55 APC (55R-286)	BioLegend	113005	B240777	FC	By manufacturer
rat anti-mouse IgG1 FITC (A85-1)	BDBiosciences	553443	92966	FC	By manufacturer
rat anti-mouse IgG2a/2b FITC (R240)	BDBiosciences	553399	4150540	FC	By manufacturer
rat anti-mouse IgG3 FITC (R40-82)	BDBiosciences	553403	7027876	FC	By manufacturer
rat anti-mouse CD138 APC (281-2)	BioLegend	142505	B237677	FC	By manufacturer
peanut agglutinin (PNA) biotin	Vector Labs	B-1075	X1221	FC	By manufacturer
mouse anti-human CD1a AlexaFlour 647 (HI149)	BioLegend	30016	B236344	FC	By manufacturer
mouse anti-human HLA-DR (L243)	BioLegend	307606	B183424	FC	By manufacturer
mouse anti-human CD45 PerCPCy5.5 (HI30)	eBiosciences	45-0459-71	E029129	FC	By manufacturer
goat anti-mouse,human Langerin (E-17)	Santa Cruz Biotechnology	sc-22620	D2216	IF	By manufacturer
rabbit anti-mouse,human active caspase-3 (polyclonal)	R&D Systems	AF835	CF23415101	IF	By manufacturer
rabbit anti-human phospho-EGFR Tyr1068 (EP774Y)	BioCare Med.	API300AA	013117	IF	By manufacturer
mouse anti-human EGFR (H11)	BioCare Med.	ACI063A	060517	IF	By manufacturer
rabbit anti-mouse phospho-EGFR Tyr1068 (D7A5)	Cell Signaling	3777S	13	FC, WB	By manufacturer and Fig. S4A,B
goat anti-mouse total EGFR (polyclonal)	R&D Systems	AF1280	HXO0216012	FC, WB	By manufacturer
rabbit anti-mouse hsp90 (polyclonal)	Cell Signaling	4874S	3	WB	By manufacturer
goat IgG polyclonal isotype control	R&D Systems	AB-108-C	ES4115041	FC,IF	By manufacturer
rat IgG2a isotype control (R35-95)	BDBiosciences	553928	4324804	FC	By manufacturer
rabbit monoclonal IgG isotype control (DA1E)	Cell Signaling	3900S	25	IF	By manufacturer
mouse IgG isotype control (#11711)	R&D	MAB002	1X12070	IF	By

	Systems		41		manufacturer
human monoclonal anti-human IgG1 ADAM17 (D1(A12))	Abcam	215268	GR3192882-1	FB, FC	By manufacturer
monoclonal human IgG1 isotype control	Adipogen	AG-35B-0006-C100	A26741504	FB, FC	By manufacturer
mouse anti-human CD3 PECy7 (UCHT1)	BioLegend	300419	B208514	FC	By manufacturer
mouse anti-human HLA-DR APC-Cy7 (L243)	BioLegend	307617	B246747	FC	By manufacturer
mouse anti-human EpCAM APC (9C4)	BioLegend	324207	B155666	FC	By manufacturer
mouse anti-human CD1a PE (BL6)	Beckman Coulter	IM1942U	11	FC	By manufacturer

Table S1. List of primary antibodies. FC= Flow Cytometry, IF= Immunofluorescence, WB= Western Blot, FB= Functional Blocking

Antibodies (Clone)	Supplier	Catalog Number	Lot Number	Application
donkey anti-goat Alexa Fluor 488 (polyclonal)	Jackson Immunoresearch	705-545-003	128611	FC
donkey anti-rabbit Alexa Fluor 647 (polyclonal)	Jackson Immunoresearch	711-606-152	125599	FC
Streptavidin Pacific Blue	ThermoFisher Scientific (Invitrogen)	S11222	1870540	FC
Streptavidin APC	ThermoFisher Scientific (Invitrogen)	S868	1124091	FC
Streptavidin Alexa Flour 488	ThermoFisher Scientific (Invitrogen)	S11223	1851449	FC, IF
donkey anti-mouse IgG biotin	Jackson Immunoresearch	715-066-151	124850	IF
donkey anti-human IgG biotin	Jackson Immunoresearch	709-066-098	135590	FC
donkey anti-rabbit rhodamine	Jackson Immunoresearch	711-295-152	130068	IF
donkey anti-goat Alexa Flour 647	Jackson Immunoresearch	705-605-147	124186	IF
donkey anti-rabbit HRP	Jackson Immunoresearch	711-035-152	128838	WB
donkey anti-goat HRP	Jackson Immunoresearch	705-035-003	130633	WB
Human TruStain FcX (Fc Receptor Blocking Solution)	BioLegend	422301	B247180	FC
DAPI	ThermoFisher Scientific (Invitrogen)	D1306	1023584	FC,IF

Table S2: Secondary antibodies and other staining reagents. FC= Flow Cytometry, IF= Immunofluorescence, WB= Western Blot